NASA TECHNICAL NOTE

NASA TN D-2324

NASA TN D-2324

VOLUME ION PRODUCTION IN A TENUOUS HELIUM PLASMA

by Ronald J. Sovie and Barry M. Klein

Lewis Research Center

Cleveland, Ohio

NATIONAL AERONAUTICS AND SPACE ADMINISTRATION • WASHINGTON, D. C. • MAY 1964

VOLUME ION PRODUCTION IN A TENUOUS HELIUM PLASMA

By Ronald J. Sovie and Barry M. Klein

Lewis Research Center
Cleveland, Ohio

NATIONAL AERONAUTICS AND SPACE ADMINISTRATION

For sale by the Office of Technical Services, Department of Commerce,
Washington, D.C. 20230 -- Price $0.75

VOLUME ION PRODUCTION IN A TENUOUS HELIUM PLASMA

by Ronald J. Sovie and Barry M. Klein

Lewis Research Center

SUMMARY

A theoretical calculation of the energy required for volume ion production has been made for a partially ionized helium plasma in which a maxwellian distribution of electron energies prevails. Inelastic electron-atom collisions that result in excitation of atomic energy levels are the only loss mechanisms considered. The energy is computed by considering the relative rates for the competing process of excitation and ionization. The results show that the energy required for volume ion production decreases sharply from 78 to 43.5 electron volts per ion as the electron kinetic temperature increases from 6 to 60 electron volts. Beyond 60 electron volts the energy required decreases slowly to 40.8 electron volts per ion at an electron kinetic temperature of 100 electron volts. The results have also been used to evaluate the ion production rate and the power consumed in ion production for a steady-state plasma as a function of electron kinetic temperature. The ion production rate and the power dissipation increase at a decreasing rate as the electron energy is increased.

INTRODUCTION

In a Joule heating device, such as a radio frequency discharge, the energy is added primarily to the electrons and is then transferred to the other species by collisions. The collisions may be either elastic or inelastic; the former result in gas heating and the latter in excitation and ionization processes. The energy transferred from the electrons in inelastic electron-atom collisions is expended usefully if the atom is ionized or is lost if the atom is excited and radiates away the excitation energy.

In plasma production and heating research it is necessary to know the net energy cost for each ion formed in the discharge, the ion production rate, and the product of these terms, which is the net power consumed in maintaining a steady-state ion density. These quantities are needed in order to determine power balances and species number densities. The purpose of this treatment is to calculate these quantities for a partially ionized, steady-state helium plasma that is optically thin and in which a maxwellian distribution of elec-

tron velocities prevails.

THEORY

Assumptions and Limitations

The volume-ion-production cost of singly ionized atoms is calculated on the basis that the only loss mechanisms present are inelastic electron-atom collisions in which atomic energy levels are excited. Elastic collisions are not considered in this analysis since the electron energy loss in elastic collisions is small compared with the energy loss in inelastic collisions for the range of electron energies considered (6 to 100 ev). All electron-atom collisions are assumed to occur with ground-state atoms. It is shown in appendix B that this is a good assumption at electron number densities much less than 10^{13} per cubic centimeter for an electron kinetic temperature of 6 electron volts. This limit increases with increasing electron kinetic temperature. Neglecting the effects of electron collisions with excited atoms will, in general, cause the calculated volume-ion-production cost to be slightly higher than the true value, since ionization of an excited state affords a means of regaining the excitation energy of that level.

The processes by which charged particles recombine may be considered separately in the ultimate power balance calculation. In the cases of wall recombination and radiative volume recombination, the energy is considered as being lost from the plasma. Although there may be an energy feedback to the electrons in three-body recombination, this is not the dominant recombination process for the range of electron energies considered (6 to 100 ev), and consequently such recombinations are neglected.

In cases where the electron kinetic temperature exceeds 40 electron volts and the percentage ionization is appreciable, collisions with excited ions and multiple ionization would have to be considered in addition to the results presented herein. This consideration is discussed in more detail in appendix B.

Development of Equations

The excitation cross section of the j^{th} atomic energy level expressed as a function of electron velocity will be represented by $\sigma_j(V_e)$. This quantity will subsequently be referred to as the excitation function of the j^{th} atomic energy level. The number of j states produced per unit volume per second by electrons with velocity V_e is given by

$$\dot{N}_j = N_0 N_e \sigma_j(V_e) V_e \qquad 1/(\text{cu cm})(\text{sec}) \tag{1}$$

(All symbols are defined in appendix A.)

If there is a distribution of electron velocities present, equation (1) must be multiplied by dN_{V_e}, the number of electrons with velocities between V_e and $V_e + dV_e$, and averaged over all velocities. Equation (1) then takes the form

$$\dot{N}_j = N_O N_e \int_{V_m}^{\infty} V_e \sigma_j(V_e) dN_{V_e} \tag{2}$$

or

$$\dot{N}_j = N_O N_e \langle \sigma(V_e)\ V_e \rangle_j \tag{3}$$

where

$$\langle \sigma(V_e) V_e \rangle_j = \int_{V_m}^{\infty} V_e \sigma_j(V_e) dN_{V_e} \tag{4}$$

The lower limit on the integral is the electron velocity corresponding to the excitation threshold energy.

For a maxwellian distribution of electron velocities,

$$dN_{V_e} = \frac{4\beta^3 V_e^2}{\sqrt{\pi}} e^{-\beta^2 V_e^2} dV_e \tag{5}$$

Equation (4) therefore becomes

$$\langle \sigma(V_e) V_e \rangle_j = \frac{4\beta^3}{\sqrt{\pi}} \int_{V_m}^{\infty} \sigma_j(V_e) V_e^3 \exp(-\beta^2 V_e^2) dV_e \tag{6}$$

Since all electron collisions are assumed to be with ground-state atoms and the energy of the j^{th} state is represented as E_j, the total energy expended per unit volume per second in exciting the j^{th} state is

$$\dot{E}_{j,tot} = \dot{N}_j E_j = N_O N_e \langle \sigma(V_e) V_e \rangle_j E_j \qquad \text{ev/(cu cm)(sec)} \tag{7}$$

If there are r states that may be excited, the total energy expended in all excitation processes is

$$\dot{E}_{exc} = \sum_{j=1}^{r} \dot{E}_j = N_0 N_e \sum_{j=1}^{r} \langle \sigma(V_e)V_e \rangle_j E_j \qquad ev/(cu\ cm)(sec) \tag{8}$$

Similarly, the number of ions formed per cubic centimeter per second is given by the relation

$$\dot{N}_{ion} = N_0 N_e \langle \sigma(V_e)V_e \rangle_{ion} \qquad 1/(cu\ cm)(sec) \tag{9}$$

Therefore,

$$\dot{E}_{ion} = N_0 N_e \langle \sigma(V_e)V_e \rangle_{ion} E_{ion} \qquad ev/(cu\ cm)(sec) \tag{10}$$

where E_{ion} is the ionization energy of the ground-state atom.

The net cost for each ion formed or the volume-ion-production cost is therefore

$$E_\varphi = \frac{\dot{E}_{ion} + \dot{E}_{exc}}{\dot{N}_{ion}} \tag{11}$$

or

$$E_\varphi = \frac{\sum_{j=1}^{r} \langle \sigma(V_e)V_e \rangle_j E_j + \langle \sigma(V_e)V_e \rangle_{ion} E_{ion}}{\langle \sigma(V_e)V_e \rangle_{ion}} \tag{12a}$$

which reduces to

$$E_\varphi = E_{ion} + \frac{\sum_{j=1}^{r} \langle \sigma(V_e)V_e \rangle_j E_j}{\langle \sigma(V_e)V_e \rangle_{ion}} \tag{12b}$$

The net power consumed in ionization processes converted to watts per cubic centimeter is

$$W = 1.602 \times 10^{-19} N_{ion} E_\varphi = 1.602 \times 10^{-19} N_0 N_e \langle \sigma(V_e)V_e \rangle_{ion} E_\varphi \qquad w/cu\ cm \tag{13}$$

where E_φ is expressed in units of electron volts per ion.

In order to evaluate E_φ (eq. (11)), $\dot{N}_{ion}$ (eq. (9)), and W (eq. (13)), the averaged excitation functions must be determined.

EXCITATION FUNCTIONS

Experimental measurements of the excitation functions of helium have been made in a number of investigations, the most notable being Lees (ref. 1) and Thieme (ref. 2). The results of these investigations may be misleading, however, since the effects of such secondary processes as imprisonment of resonance radiation, cascading, and excitation transfer were not subtracted from the measured cross sections. The experiments of reference 2 were performed at a lower pressure than those of reference 1. Consequently, the results of reference 2 would be expected to possess a greater degree of accuracy since the extent to which these secondary processes affect the cross-section determination increases with pressure. Phelps (ref. 3) has applied the theory of imprisonment of resonance radiation to measurements of excitation cross sections. The results of reference 3 have been considered by Gabriel and Heddle (ref. 4) in their investigation of helium excitation cross sections at 108 electron volts, and they have also applied corrections for cascading and excitation transfer effects. It is pointed out by Frost and Phelps in reference 4 that the excitation functions of reference 2 for members of the same spectral series have very nearly the same shape and may be represented as the product of a shape function $g(V_e)$ and some magnitude, which may conveniently be taken as the maximum cross section. The experiments of reference 2 were performed at a low pressure (5 microns), and although the magnitudes of some of the cross sections are in error, the shape functions obtained should be close to the true shape functions within the experimental error. The only exceptions are the 3^1P level and the n^3P series, for which cascading effects must be considered. The corrected shape functions for these levels are given by

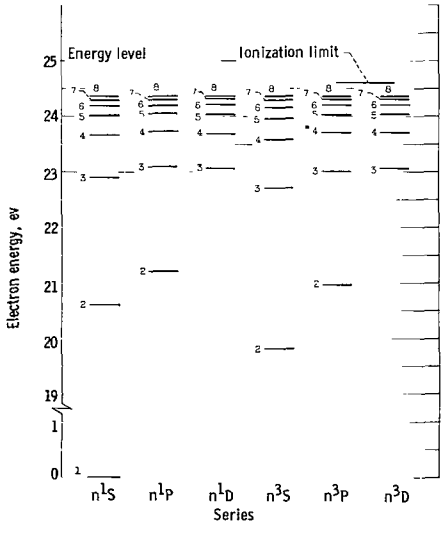

Figure 1. - Energy-level diagram for helium.

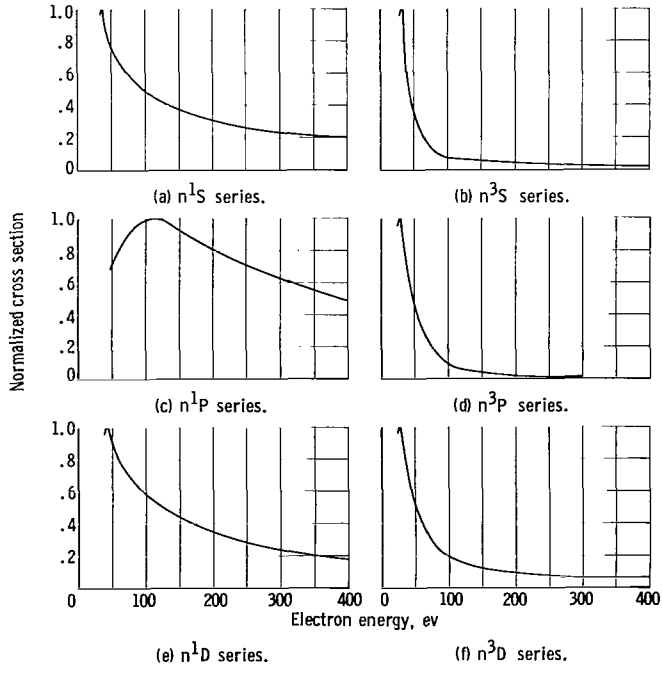

Figure 2. - Normalized excitation shape functions.

Gabriel and Heddle (ref. 4).

Only the first eight energy levels of each series were considered pertinent in the calculation of the volume-ion-production cost, and they are shown in figure 1. The shape functions used for the various spectral series are those of reference 2, with the previously mentioned corrections being made for cascading effects. The shape functions are shown in figure 2 normalized to

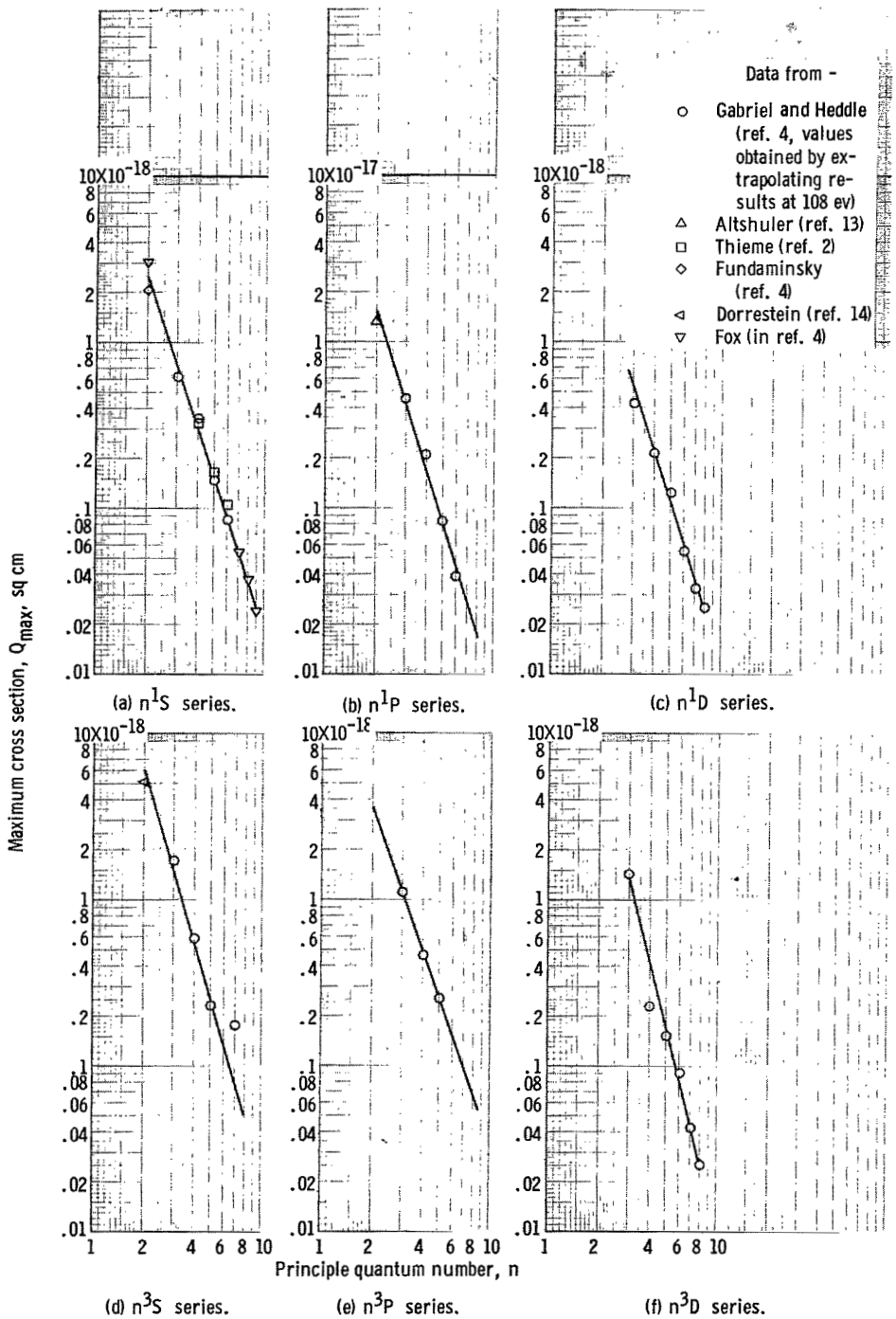

Figure 3. - Maximum excitation cross sections.

unity at their maximum value. Gabriel and Heddle obtained the maximum cross sections by fitting their results at 108 electron volts to these shape functions. The Q_{max} values are presented in figure 3 as a function of principal quantum number. A presentation of this type was first suggested by Frost and Phelps in reference 4, which shows that data from that study can be represented by $Q_{max} \propto n^{-\alpha}$, where α varies from 3 to 3.5. In reference 4 it is stated that a reasonable presentation of the data obtained would be $Q_{max} \propto (n^*)^{-3}$, where n^* is the effective principal quantum number defined as the reciprocal of the square root of the term value in rydbergs. Hartree, reference 5, has shown that the intensities of the spectral lines of a given spectral series might be expected to follow a $(n^*)^{-3}$ law, and similar behavior would be expected of the excitation cross sections. This determination of the maximum cross sections allows for the effects of secondary processes, and these values agree quite well with those of reference 2 for levels in which the data (ref. 2) are not in error because of the effects of secondary processes.

For the purpose of comparison, the results of a number of independent calculations of maximum cross sections are also shown in figure 3. Cross sections for levels that were not experimentally determined in reference 4 are obtained by extrapolation of this figure. The shape functions and the maximum values used in figures 2 and 3 are considered to be accurate to within ±10 percent (ref. 4).

As a final check on the magnitude of the excitation functions, the total inelastic excitation cross section is calculated by using the previous results and is plotted as a function of electron energy in figure 4. The ionization and elastic cross sections are also presented in this figure. The sum of these cross sections is then compared with the experimental total cross sections of

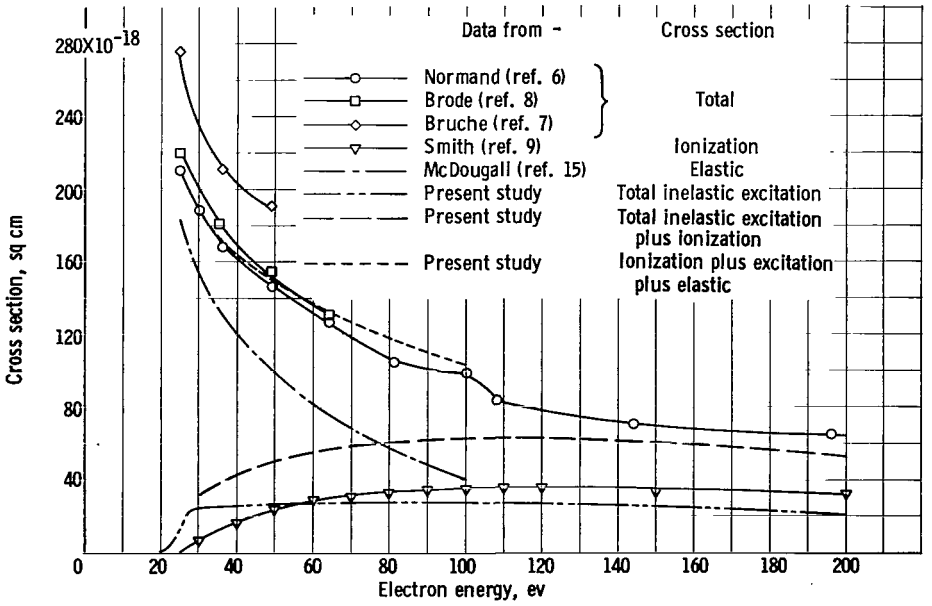

Figure 4. - Cross-section comparison.

Normand (ref. 6), Bruche (ref. 7), and Brode (ref. 8). It is seen in figure 4 that except for the results of reference 7 good agreement is obtained between the sum of the individual cross sections and the experimental total cross sections.

DETERMINATION OF $\langle \sigma(V_e)V_e \rangle_j$ AND RESULTS

The shape functions presented in the previous section are represented by empirical equations giving the cross section as a function of electron velocity. The empirical fits to the shape functions are shown in figure 5. These empirical equations are multiplied by the electron velocity and are averaged over a maxwellian velocity distribution to obtain the $\langle \sigma(V_e)V_e \rangle_j$ quantities. The equations used, their range of validity, and the form of the $\langle \sigma(V_e)V_e \rangle_j$ quantities are listed in table I, while table II contains the numerical values of the constants used for each of the levels considered. The empirical fits to the excitation functions are considered accurate to within ±10 percent of the experimental curves. For the purpose of expediting the calculation of the $\langle \sigma(V_e)V_e \rangle_j$ quantities listed in tables I and III, the units of V_m, V_e, and V_{number} are chosen for this case to be the square root of electron volts per gram so that βV_m and βV_e are dimensionless quantities. The constant γ appears in tables I and III in order to convert the $\langle \sigma(V_e)V_e \rangle_j$ quantities to units of cubic centimeters per second.

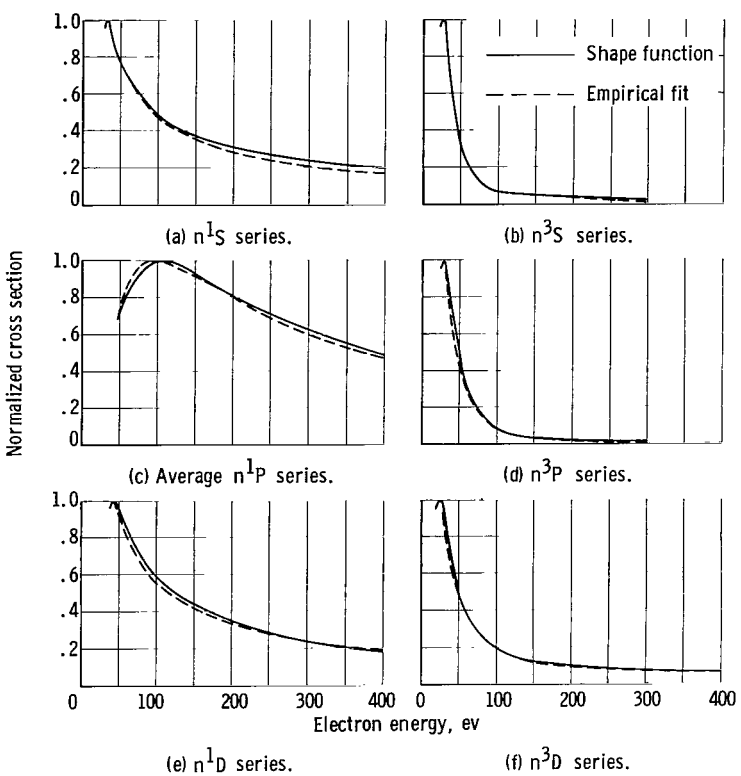

Figure 5. - Comparison of empirical fits with normalized shape functions.

The ionization cross section used in the calculation of the $\langle \sigma(V_e)V_e \rangle_{ion}$ quantity was from Smith (ref. 9). The empirical fit for this cross section is shown in figure 6, and the other relevant data concerning this fit are presented in table III.

TABLE I. - PARAMETRIC EQUATIONS AND $\langle\sigma(V_e)V_e\rangle$ RELATIONS

Series	Parametric equation for, $\sigma(V_e)$	Energy range, ev	Maxwellian averaged cross section, $\langle\sigma(V_e)V_e\rangle$
n^1S	$\tau V_e^2 - A_1$	$E_m \le E \le 35$	$\frac{2\gamma}{\sqrt{\pi}\beta}\left\{\exp(-\beta^2V_e^2)\left[\frac{2\tau}{\beta^2}\left(1+\beta^2V_e^2+\frac{\beta^4V_e^4}{2}\right)-A_1(1+\beta^2V_e^2)\right]\right\}\Bigg\vert_{V_e=V_m}^{V_e=V_{35}}$
	$\frac{K}{V_e^{3/2}}$	$35 \le E \le \infty$	$+\frac{2}{\sqrt{\pi}}\beta^{1/2}K\gamma\Gamma_{\beta^2V_{35}^2}\left(\frac{5}{4}\right)$
n^1P	$\frac{A_1V_m^2(V_e-V_m)^2}{V_e^4}$	$E_m \le E \le 200$	$\frac{4\beta^3}{\sqrt{\pi}}A_1V_m^2\gamma\left\{\frac{1}{2\beta^2}\exp(-\beta^2V_e^2)-\frac{\sqrt{\pi}}{\beta}V_m[\operatorname{erfc}(\beta V_e)]-\frac{V_m^2}{2}\operatorname{Ei}(-\beta^2V_e^2)\right\}\Bigg\vert_{V=V_m}^{V=V_{200}}$
	$\frac{K}{V_e^{3/2}}$	$200 \le E \le \infty$	$+\frac{2}{\sqrt{\pi}}\beta^{1/2}K\gamma\Gamma_{\beta^2V_{200}^2}\left(\frac{5}{4}\right)$
n^1D	$A_1\left(1-\frac{V_m}{V_e}\right)$	$E_m \le E \le 45$	$A_1\gamma\left\{\frac{2}{\beta\sqrt{\pi}}(1+\beta^2V_e^2-\beta^2V_mV_e)\exp(-\beta^2V_e^2)-V_m[\operatorname{erfc}(\beta V_e)]\right\}\Bigg\vert_{V_e=V_m}^{V_e=V_{45}}$
	$\frac{K}{V_e^{3/2}}$	$45 \le E \le \infty$	$+\frac{2}{\sqrt{\pi}}\beta^{1/2}K\gamma\Gamma_{\beta^2V_{45}^2}\left(\frac{5}{4}\right)$
n^3S	$\tau V_e^2 - A_1$	$E_m \le E \le 28$	$\frac{2}{\sqrt{\pi}}\frac{\gamma}{\beta}\left\{\exp(-\beta^2V_e^2)\left[\frac{2\tau}{\beta^2}\left(1+\beta^2V_e^2+\frac{\beta^4V_e^4}{2}\right)-A_1(1+\beta^2V_e^2)\right]\right\}\Bigg\vert_{V_e=V_m}^{V_e=V_{28}}$
	$\frac{C}{V_e^4}$	$28 \le E \le \infty$	$-\frac{2}{\sqrt{\pi}}\beta^3C\gamma\operatorname{Ei}(-\beta^2V_{28}^2)$
n^3P	$\tau V_e^2 - A_1$	$E_m \le E \le 32$	$\frac{2}{\sqrt{\pi}}\frac{\gamma}{\beta}\left\{\exp(-\beta^2V_e^2)\left[\frac{2\tau}{\beta^2}\left(1+\beta^2V_e^2+\frac{\beta^4V_e^4}{2}\right)-A_1(1+\beta^2V_e^2)\right]\right\}\Bigg\vert_{V_e=V_m}^{V_e=V_{32}}$
	$\frac{C}{V_e^4}$	$32 \le E \le \infty$	$-\frac{2}{\sqrt{\pi}}\beta^3C\gamma\operatorname{Ei}(-\beta^2V_{32}^2)$
n^3D	$\tau V_e^2 - A_1$	$E_m \le E \le 28$	$\frac{2}{\sqrt{\pi}}\frac{\gamma}{\beta}\left\{\exp(-\beta^2V_e^2)\left[\frac{2\tau}{\beta^2}\left(1+\beta^2V_e^2+\frac{\beta^4V_e^4}{2}\right)-A_1(1+\beta^2V_e^2)\right]\right\}\Bigg\vert_{V_e=V_m}^{V_e=V_{28}}$
	$\frac{Z}{V_e^{5/2}}$	$28 \le E \le 200$	$+\frac{8}{3\sqrt{\pi}}Z\beta^3\gamma\left[\frac{1}{\beta^{3/2}}\Gamma_{\beta^2V_e^2}\left(\frac{7}{4}\right)-V_e^{3/2}\exp(-\beta^2V_e^2)\right]\Bigg\vert_{V=V_{28}}^{V=V_{200}}$
	$\frac{H}{V_e}$	$200 \le E \le \infty$	$+\gamma H\left[\operatorname{erfc}(\beta V_{200})+\frac{2\beta V_{200}}{\sqrt{\pi}}\exp(-\beta^2V_{200}^2)\right]$

TABLE II. - NUMERICAL VALUES OF CONSTANTS FOR PARAMETRIC FITS TO EXCITATION FUNCTIONS

Principal quantum number, n	Series									
	1_S			1_P		1_D		3_S		
	$\tau \times 10^{-48}$	$A_1 \times 10^{-20}$	$K \times 10^{3}$	$A_1 \times 10^{-17}$	$K \times 10^{4}$	$A_1 \times 10^{-19}$	$K \times 10^{3}$	$\tau \times 10^{-48}$	$A_1 \times 10^{-20}$	$C \times 10^{39}$
2	82.7	375.9	11.98	24.96	21.44	------	-----	355.1	1459	22.85
3	23.7	119.5	2.91	7.321	6.28	15.30	2.42	145.5	726.2	6.36
4	14.11	73.39	1.63	3.374	2.888	7.97	1.216	58.81	304.9	2.155
5	6.361	33.27	.703	1.351	1.155	4.82	.719	25.5	134.4	.851
6	3.65	19.71	.402	.628	.536	1.56	.304	21.92	115.6	.722
7	2.231	11.88	.245	.483	.4125	1.233	.182	20.7	110.2	.635
8	1.564	8.23	.171	.273	.2406	.962	.142	5.91	31.5	.1816

Principal quantum number, n	Series						
	3_P			3_D			
	$\tau \times 10^{-48}$	$A_1 \times 10^{-20}$	$C \times 10^{39}$	$\tau \times 10^{-48}$	$A_1 \times 10^{-20}$	$Z \times 10^{17}$	$H \times 10^{-6}$
2	160	736.1	19.2	-------	------	------	-----
3	56.8	287.3	5.55	135	683.7	14.1	82.1
4	25.85	135.5	2.356	24.97	129.4	2.32	12.96
5	14.95	78.90	1.292	17.31	91.38	1.45	8.55
6	8.59	45.5	.7419	10.99	49.26	.881	5.12
7	5.55	29.8	.475	5.235	27.94	.41	2.38
8	3.736	19.87	.3165	3.089	16.48	.242	1.416

TABLE III. - PARAMETRIC EQUATIONS FOR IONIZATION CASE

[$A_1 = 4.878 \times 10^{-17}$ sq cm; $A_2 = 3.93 \times 10^{-17}$ sq cm; $G = 12.50 \times 10^{42}$ $(ev/g)^{3/2}$; $A_3 = 4.010 \times 10^{-17}$ sq cm; $\tau = 1.89 \times 10^{-47}$ (g)(sq cm)/ev; $H = 20.68 \times 10^{-3}$ sq cm $(ev/g)^{1/2}$]

Parametric equation for, $\sigma(V_e)$	Energy range, ev	Maxwellian averaged cross section, $\langle \sigma(V_e)V_e \rangle$
$A_1\left(1 - \frac{V_m^2}{V_e^2}\right)$	$E_m \leq E \leq 62$	$\frac{2A_1\gamma}{\beta\sqrt{\pi}} \left[(1 + \beta^2 V_e^2) - \beta^2 V_m^2\right] \exp(-\beta^2 V_e^2) \Big\|_{V_e=V_m}^{V_e=V_{62}}$
$A_2\left(1 - \frac{G}{V_e^3}\right)$	$62 \leq E \leq 116$	$+ \frac{2A_2\gamma}{\beta\sqrt{\pi}} \left\{\exp(-\beta^2 V_e^2)(1 + \beta^2 V_e^2) - 2\beta^2 A_2 G \left[\operatorname{erfc}(\beta V_e)\right]\right\} \Big\|_{V=V_{116}}^{V=V_{62}}$
$A_3 - \tau V_e^2$	$116 \leq E \leq 480$	$+ \frac{2\gamma}{\beta\sqrt{\pi}} \exp(-\beta^2 V_e^2) \left[A_3(1 + \beta^2 V_e^2) - \frac{2\tau}{\beta^2}\left(1 + \beta^2 V_e^2 + \frac{\beta^4 V_e^4}{2}\right)\right] \Big\|_{V=V_{480}}^{V=V_{116}}$
$\frac{H}{V_e}$	$480 \leq E \leq \infty$	$+ H\gamma \left[\operatorname{erfc}(\beta V_{480}) + \frac{2\beta V_{480}}{\sqrt{\pi}} \exp(-\beta^2 V_{480}^2)\right]$

The $\langle \sigma(V_e)V_e \rangle_j$ quantities shown in tables I and III are multiplied by the appropriate energy values as obtained from Moore (ref. 10) and the volume-ion-production cost is then determined from equation (12). The cost in electron volts for each ion is presented in figure 7 as a function of electron kinetic temperature. The cost decreases sharply from 78 to 43.5 electron volts per ion as the electron kinetic temperature increases from 6 to 60 electron volts. Beyond 60 electron volts the cost decreases slowly to 40.8 electron volts per ion

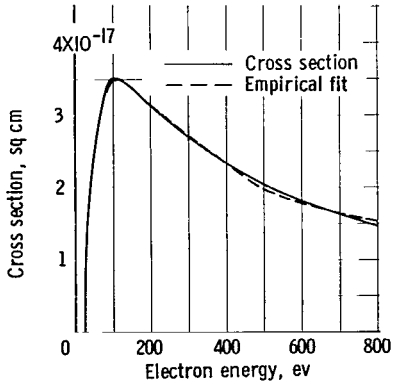

Figure 6. - Comparison of empirical fit with ionization cross section.

at an electron kinetic temperature of 100 electron volts. An inspection of the ionization and the total inelastic-excitation cross sections in figure 4 shows that the shape of the cost curve is as expected, since at low temperatures excitation is more probable than ionization, and the reverse is true at high temperatures. It should be pointed out again, however, that inelastic collisions with ions have not been considered in this treatment. If these collisions were considered, the curve of the volume-ion-production cost would begin to increase at approximately 40 electron volts and would reach a maximum value at some high electron kinetic temperature.

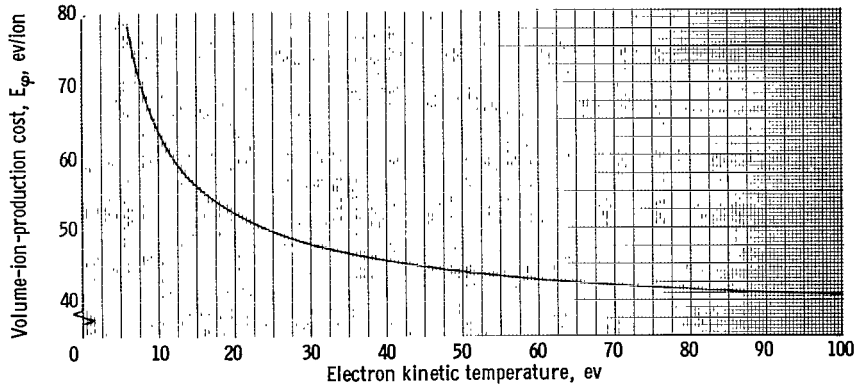

Figure 7. - Volume-ion-production cost as function of electron kinetic temperature.

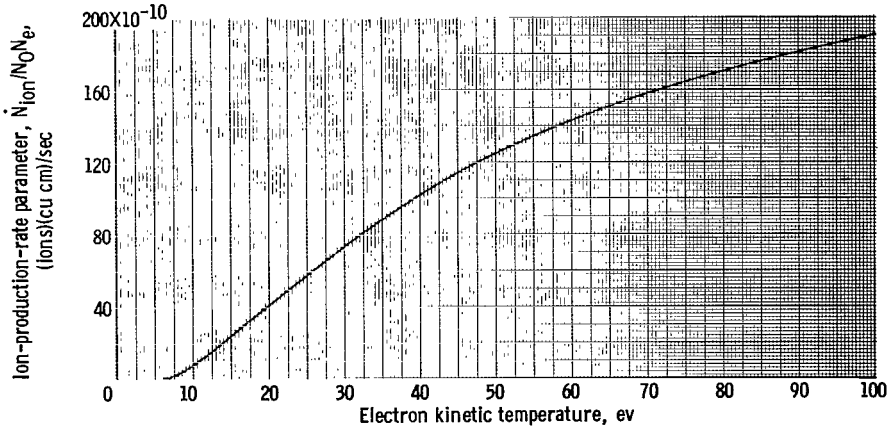

Figure 8. - Ion-production-rate parameter as function of electron kinetic temperature.

In order to facilitate the use of these results in other calculations, such as a power balance, two additional curves are presented. An ion-production-rate parameter $\dot{N}_{ion}/N_0N_e$ (eq. (9)) is plotted as a function of electron kinetic temperature in figure 8, and figure 9 shows the variation of

the power consumed in ion production $E_{\varphi}(\dot{N}_{ion}/N_0N_e)$ (eq. (13)) with electron kinetic temperature.

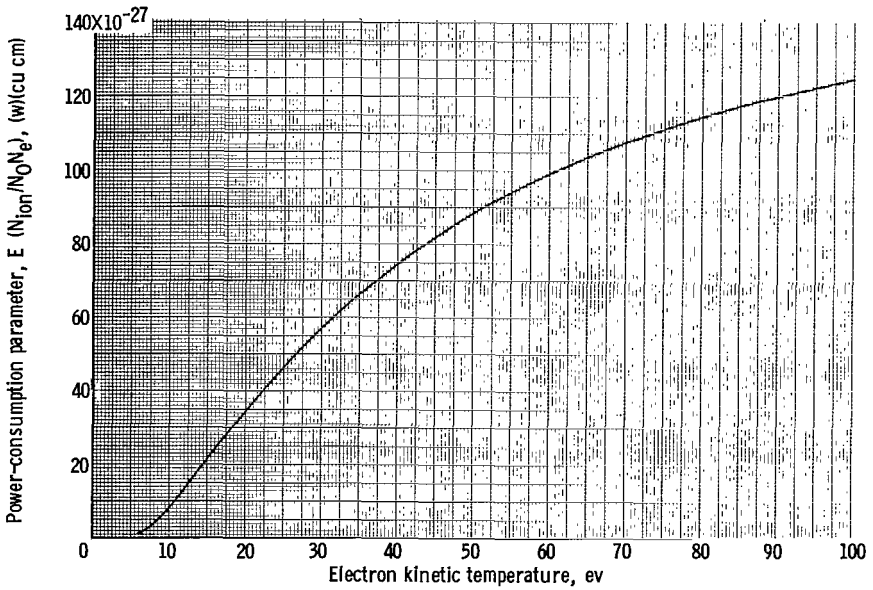

Figure 9. - Power-consumption parameter as function of electron kinetic temperature.

In order to obtain the ion-production rate and the power consumed in ion production for any experiment, all that is needed is to multiply the rate and power parameters by the N_0N_e ($1/cm^6$) and by the volume in cubic centimeters appropriate to that experiment. The results presented in figures 7 to 9 are tabulated in table IV.

CONCLUDING REMARKS

The results of a number of individual investigations of helium excitation functions have been combined to generate a credible self-consistent set of helium excitation functions. These excitation functions have been used to calculate the volume-ion-production cost for a helium plasma. This cost decreases sharply from 78 to 43.5 electron volts per ion as the electron kinetic temperature increases from 6 to 60 electron volts. Beyond 60 electron volts the cost decreases slowly to 40.8 electron volts per ion at any electron energy of 100 electron volts.

The ion-production rate and the required power dissipation for a steady-state plasma were also evaluated as functions of electron energy. These quantities increase at a decreasing rate as the electron kinetic temperature is increased. Because of the experimental uncertainty in determining the excitation functions and the percentage errors encountered in the empirical fits, the results presented in this report are considered accurate to within ±20 percent of the true values. The results apply to a steady-state, partially ion-

TABLE IV. - CALCULATED RESULTS

Electron kinetic temperature, ev	Ion-production cost, E_φ, ev/ion	Ion-production rate, $\frac{\dot{N}_{ion}}{N_O N_e}$, (ions)(cu cm)/sec	Power dissipated in producing ions, $E_\varphi \frac{\dot{N}_{ion}}{N_O N_e}$, (watt)(cu cm)
6	77.8	1.3×10^{-10}	1.7×10^{-27}
8	68.8	4.3	4.7
12	59.7	14.5	13.9
16	55.1	27.8	24.5
20	52.1	41.8	34.9
24	50.0	55.6	44.6
28	48.5	68.7	53.4
32	47.4	80.8	61.4
36	46.4	92.1	68.5
40	45.7	102.5	75.0
44	45.0	112.1	80.8
48	44.5	120.9	86.1
52	44.0	129.0	90.9
56	43.6	136.5	95.2
60	43.2	143.4	99.2
64	42.8	149.8	102.8
68	42.5	155.8	106.1
72	42.2	161.3	109.1
76	42.0	166.4	111.9
80	41.7	171.1	114.4
84	41.5	175.6	116.8
88	41.3	179.7	118.9
92	41.1	183.6	121.0
96	41.0	187.2	122.8
100	40.8	190.6	124.5

ized helium plasma that is optically thin and in which a maxwellian distribution of electron velocities prevails. If, however, the electron temperature and density are such that the appropriate steady-state ionization equation (corrected Saha or corona equation) predicts an appreciable degree of ionization, the presented results are valid only if the ionization and excitation are reduced by enhanced recombination and deexcitation effects, for example, at the walls of a discharge chamber. It should be noted that the results presented herein would represent one term in a power or species balance calculation, that is, the ion-production rate or the power dissipated in ion production. There will be additional terms to account for recombination and wall losses, but these will be different for different experimental configurations and are therefore not included in this calculation. There will also be additional power requirements if the plasma is heated, accelerated, or performs work.

Lewis Research Center
National Aeronautics and Space Administration
Cleveland, Ohio, January 2, 1964

APPENDIX A

SYMBOLS

A_1, A_2, A_3	quantities used in parametric equations, sq cm
C	quantity used in parametric equations, $\left[(\text{cm})(\text{ev})/\text{g}\right]^2$
D	spectral level with angular momentum corresponding to L = 2
E	energy, ev
E_{ion}	ionization energy, ev
Ei(-x)	$-\int_x^\infty e^{-y}/y \, dy$
E_j	energy of j^{th} atomic energy level, ev
E_m	threshold energy for exciting a level
E_φ	volume-ion-production cost, ev/ion
$\dot{E}_{exc}$	energy expended in excitation processes, ev/(cu cm)(sec)
$\dot{E}_{ion}$	energy expended in ionization processes, ev/(cu cm)(sec)
$\dot{E}_{j,tot}$	total energy expended in exciting j^{th} atomic energy level, ev/(cu cm)(sec)
E_+	excitation energy of ion energy levels
erf(x)	$\frac{2}{\sqrt{\pi}}\int_x^\infty e^{-y} \, dy$
erfc(x)	1 - erf(x)
G	quantity used in parametric equations, $(\text{ev/g})^{3/2}$
$g(V_e)$	shape function for spectral series
H	quantity used in parametric equations, $(\text{sq cm})(\text{ev/g})^{1/2}$
j	j^{th} atomic energy level
K	quantity used in parametric equations, $(\text{ev/g})^{3/4}$

kT_e	electron kinetic temperature, ev
m_e	electron mass, g
N_e	electron density, electrons/sq cm
N_{ion}	ion density, ions/cu cm
$\dot{N}_M$	metastable production rate, metastables/(cu cm)(sec)
N_0	neutral density, atoms/cu cm
$\dot{N}_{IM}$	production rate of ions from metastable state, ions/(cu cm)(sec)
$\dot{N}_{ion}$	ion production rate, ions/(cu cm)(sec)
$\dot{N}_j$	j^{th} state production rate, 1/(cu cm)(sec)
n	principal quantum number
n^*	effective principal quantum number
P	spectral level with angular momentum corresponding to L = 1
Q_{max}	maximum cross section, sq cm
R	$\dot{N}_{IM}/\dot{N}_{ion}$
r	number of energy levels considered
S	spectral level with angular momentum corresponding to L = 0
V_e	electron velocity, cm/sec or $(ev/g)^{1/2}$
V_m	electron velocity corresponding to threshold energy for exciting a level, cm/sec or $(ev/g)^{1/2}$
V_{number}	electron velocity corresponding to energy used as limit in averaging process, $(ev/g)^{1/2}$
W	power, w
x, y	coordinates
Z	quantity used in parametric equations, (sq cm)$(ev/g)^{5/4}$
β	$(m_e/2kT_e)^{1/2}$, $(g/ev)^{1/2}$
$\Gamma_{\beta^2V_e^2}(\tau)$	$\int_{\beta^2V_e^2}^{\infty} e^{-y} y^{\tau-1}\, dy$, incomplete gamma function

γ	$1.266\times10^{-6}\left[(\text{sq cm})(\text{g})/(\text{sec}^2)(\text{ev})\right]^{1/2}$
$\sigma(V_e)$	excitation function for an atomic energy level, sq cm
$\sigma_{IM}(V_e)$	ionization function for metastable helium atom, sq cm
$\sigma_{ion}(V_e)$	ionization function for helium atom, sq cm
$\sigma_j(V_e)$	excitation function for j^{th} atomic energy level, sq cm
$\sigma_+(V_e)$	excitation function for helium II energy levels
τ	quantity used in parametric equations, (sq cm)(g)/ev
τ_M	lifetime of metastable state, sec

Superscripts:

1	singlet state
3	triplet state

APPENDIX B

LIMITATIONS OF ASSUMPTIONS

Electron-Excited-Atom Interactions

The interaction between electrons and excited atoms that would have the greatest effect on the calculations would be the ionization of helium in a metastable state, since the metastable states have a lifetime of approximately 10^{-6} second, which is roughly two orders of magnitude greater than the lifetimes of ordinary excited states. In order to justify neglecting these processes in the calculation of the volume-ion-production cost, it must be shown that the ratio of the number of metastable atoms ionized per second to the number of ground-state atoms ionized per second is very much less than 1. In equation form,

$$R = \frac{\dot{N}_{IM}}{\dot{N}_{ion}} \ll 1 \tag{B1}$$

The number of metastable atoms ionized per second is given by the relation

$$\dot{N}_{IM} = \dot{N}_M N_e \tau_M \langle \sigma(V_e) V_e \rangle_{IM} \tag{B2}$$

where

$$\dot{N}_M = N_0 N_e \langle \sigma(V_e) V_e \rangle_M \tag{B3}$$

Similarly,

$$\dot{N}_{ion} = N_0 N_e \langle \sigma(V_e) V_e \rangle_{ion} \tag{B4}$$

Consequently, equation (B1) becomes

$$R = \frac{N_0 N_e \langle \sigma(V_e) V_e \rangle_M N_e \tau_M \langle \sigma(V_e) V_e \rangle_{IM}}{N_0 N_e \langle \sigma(V_e) V_e \rangle_{ion}} \ll 1 \tag{B5}$$

or

$$R = \frac{\tau_M N_e \langle \sigma(V_e) V_e \rangle_M \langle \sigma(V_e) V_e \rangle_{IM}}{\langle \sigma(V_e) V_e \rangle_{ion}} \ll 1 \tag{B6}$$

Considering, for example, the helium 2^1S metastable state, calculations for an electron kinetic temperature of 20 electron volts show that

$$\langle \sigma(V_e) V_e \rangle_{M2^1S} = 3.82 \times 10^{-10} \text{ cu cm/sec}$$

and

$$\langle \sigma(V_e)V_e \rangle_{ion} = 4.18\times10^{-9} \text{ cu cm/sec}$$

The cross section for ionization of a helium 2^1S metastable atom has not been determined experimentally, but a calculation using the Gryzinski method (ref. 11) indicates that the maximum value of $\langle \sigma(V_e)V_e \rangle_{IM2^1S}$ would be approximately 6×10^{-7} cubic centimeter per second. Substituting these quantities into (B6) yields

$$R = \frac{10^{-6}(3.82\times10^{-10})(6\times10^{-7})}{4.18\times10^{-9}} N_e \ll 1$$

$$= 5.48\times10^{-14} N_e \ll 1$$

Consequently, the approximation is good for

$$N_e \ll 1.81\times10^{13} \text{ cu cm}$$

At an electron temperature of 6 electron volts a similar calculation indicates that 10^{13} per cubic centimeter would represent an approximate upper bound on the electron density. It should be noted that these estimates are on the conservative side, and the upper bound increases as the electron temperature is increased beyond 20 electron volts.

Electron-Ion Interactions

Consider the case where the helium ions may be excited but not ionized. The equation for the net energy cost for each ion produced then takes the form

$$E_\varphi = \frac{\sum_j \langle \sigma(V_e)V_e \rangle_j E_j}{\langle \sigma(V_e)V_e \rangle_{ion}} + \frac{N_{ion}}{N_0} \frac{\langle \sigma(V_e)V_e \rangle_+ E_+}{\langle \sigma(V_e)V_e \rangle_{ion}} \tag{B7}$$

where the summation over j includes the ionization of the neutral atom. The effects of exciting the helium II states are negligible if

$$\frac{\sum_j \langle \sigma(V_e)V_e \rangle_j E_j}{\frac{N_{ion}}{N_0} \langle \sigma(V_e)V_e \rangle_+ E_+} \gg 1 \tag{B8}$$

The threshold energy for an $n = 1$ to $n = 2$ excitation in helium II is 40.6 electron volts. This is the most probable excitation in helium II, and at an electron kinetic temperature of 40 electron volts ionization of helium II may be neglected since the threshold for ionization is 54 electron volts.

For an electron kinetic temperature of 40 electron volts, calculations show that

$$\sum_j \langle \sigma(V_e)V_e \rangle_j E_j \cong 37\times10^{-2} \qquad \text{ev/(g)(sq cm)}$$

$$\langle \sigma(V_e)V_e \rangle_{1\text{-}2+} E_{2+} \cong 3\times10^{-2} \qquad \text{ev/(g)(sq cm)}$$

The $\langle \sigma(V_e)V_e \rangle_{1\text{-}2+} E_{2+}$ value was obtained by using the approximation for this cross section given by Berger (ref. 12). Substituting these values into (B8) yields

$$\frac{37\times10^{-2}}{\frac{N_{ion}}{N_0}(3\times10^{-2})} \gg 1$$

or

$$\frac{12.3}{\frac{N_{ion}}{N_0}} \gg 1$$

Thus, for the case considered the excitation of helium II levels may be neglected for a range of N_{ion}/N_0 values. The effect of the excitation of helium II energy levels will decrease with decreasing electron kinetic temperature. If there is an appreciable amount of ionization and if the electron kinetic temperature increases beyond 40 electron volts, the effects of excitation and ionization of the helium ion will become increasingly important and will have to be considered along with the results presented in this report.

REFERENCES

1. Lees, J. H.: Excitation Function of Helium. Proc. Roy. Soc. (London), ser. A, vol. 137, 1932, pp. 173-186.

2. Thieme, Otto: Lichtausbeute in Helium, Quecksilber-und Stickstoffspektrum bei Anregung durch Electronenstosz. (Efficiency of Excitation by Electron Impact in the Spectra of Helium, Mercury, and Nitrogen.) Z. Physik 78, 1932, pp. 412-422.

3. Phelps, A. V.: Effect of the Imprisonment of Resonance Radiation on Excitation Experiments. Phys. Rev., vol. 110, no. 6, June 1958, pp. 1362-1368.

4. Gabriel, A. H., and Heddle, D. W. O.: Excitation Processes in Helium. Proc. Roy. Soc. (London), ser. A, vol. 258, 1960, pp. 124-145.

5. Hartree, D. R.: Wave Mechanics of an Atom with a Non-Coulomb Central Field. III. Term Values and Intensities in Series in Optical Spectra. Proc. Cambridge Phil. Soc., vol. 24, pt. 3, 1928, pp. 426-437.

6. Normand, C. E.: The Absorption Coefficient for Slow Electrons in Gases. Phys. Rev., vol. 35, May 1930, pp. 1217-1225.

7. Bruche, Ernest, Lilienthal, Dorothee, and Schordter, Kate: Effective Cross Sections of the Rare Gases Argon, Neon and Helium Toward Slow Electrons. Ann. Physik, vol. 84, Oct. 1927, pp. 279-291.

8. Brode, R. B.: Absorption Coefficient for Slow Electrons in Gases. Phys. Rev., vol. 25, 1925, pp. 636-644.

9. Smith, Philip T.: The Ionization of Helium, Neon, and Argon by Electron Impact. Phys. Rev., vol. 36, Oct. 1930, pp. 1293-1302.

10. Moore, Charlotte E.: Atomic Energy Levels. NBS Circular 467, 1949, pp. 4-6.

11. Gryzinski, Michal: Classical Theory of Electronic and Ionic Inelastic Collisions. Phys. Rev., vol. 115, no. 2, July 1959, pp. 374-383.

12. Berger, J. M. and Friedman, E. A.: On the Pulse Method of Ionization and Heating of a Plasma. NYO (AEC) 6043, 1953.

13. Altshuler, Saul: Excitation Cross Section for Helium Atoms. II. Phys. Rev., vol. 89, no. 5, March 1953, p. 1093-1095.

14. Dorrestein, R.: Anregungsfunktionen Metastabiler Zustande in Helium and Neon, Gemessen mit Hilfe Der Von Metastagilen Atomen Verursachten Electronen Auslosung Aus Metallen. (Excitation of Metastable States in Helium and Neon Measured by Means of Electron Emission from Metals Caused by Metastable Atoms.) Physica, vol. 9, 1942, pp. 447-459.

15. McDougall, J.: Motion of Electrons in the Static Fields of Hydrogen and Helium. Proc. Roy. Soc. (London), ser. A, vol. 136, 1932, pp. 549-558.

"The National Aeronautics and Space Administration . . . shall . . . provide for the widest practical appropriate dissemination of information concerning its activities and the results thereof . . . objectives being the expansion of human knowledge of phenomena in the atmosphere and space."

—National Aeronautics and Space Act of 1958

NASA SCIENTIFIC AND TECHNICAL PUBLICATIONS

TECHNICAL REPORTS: Scientific and technical information considered important, complete, and a lasting contribution to existing knowledge.

TECHNICAL NOTES: Information less broad in scope but nevertheless of importance as a contribution to existing knowledge.

TECHNICAL MEMORANDUMS: Information receiving limited distribution because of preliminary data, security classification, or other reasons.

CONTRACTOR REPORTS: Technical information generated in connection with a NASA contract or grant and released under NASA auspices.

TECHNICAL TRANSLATIONS: Information published in a foreign language considered to merit NASA distribution in English.

TECHNICAL REPRINTS: Information derived from NASA activities and initially published in the form of journal articles or meeting papers.

SPECIAL PUBLICATIONS: Information derived from or of value to NASA activities but not necessarily reporting the results of individual NASA-programmed scientific efforts. Publications include conference proceedings, monographs, data compilations, handbooks, sourcebooks, and special bibliographies.

Details on the availability of these publications may be obtained from:

SCIENTIFIC AND TECHNICAL INFORMATION DIVISION

NATIONAL AERONAUTICS AND SPACE ADMINISTRATION

Washington, D.C. 20546